LAWRENCE
LIVERMORE
NATIONAL
LABORATORY

LLNL-JRNL-647352

Thomson scattering from a three-component plasma

W. R. Johnson, J. Nilsen

December 6, 2013

Physical Review E

Disclaimer

Thomson scattering from a three-component plasma

W. R. Johnson*
Department of Physics, 225 Nieuwland Science Hall
University of Notre Dame, Notre Dame, IN 46556

J. Nilsen
Lawrence Livermore National Laboratory, Livermore CA 94551

A model for a three-component plasma consisting of two distinct ionic species and electrons is developed and applied to study X-ray Thomson scattering. Ions of a specific type are assumed to be identical and are treated in the average-atom approximation. Given the plasma temperature and density, the model predicts mass-densities, effective ionic charges and cell volumes for each ionic type, together with the plasma chemical potential and free electron density. Additionally, the average-atom treatment of individual ions provides a quantum-mechanical description of bound and continuum electrons. The model is used to obtain parameters needed to determine the dynamic structure factors for X-ray Thomson scattering from a three-component plasma. The contribution from inelastic scattering by free electrons is evaluated in the random-phase approximation. The contribution from inelastic scattering by bound electrons is evaluated using the bound-state and scattering wave functions obtained from the average-atom calculations. Finally, the partial static structure factors for elastic scattering by ions are evaluated using a two-component version of the Ornstein-Zernike equations with hypernetted chain closure, in which electron-ion interactions are accounted for using screened ion-ion interaction potentials. The model is used to predict the X-ray Thomson scattering spectrum from a CH plasma and the resulting spectrum is compared with experimental results obtained by Feltcher *et al.*, Phys. Plasmas, **20**, 056316 (2013).

PACS numbers: 52.65.Rr, 52.27.Cm, 52.70.-m, 52.38.-r, 52.25.Os, 52.27.Gr,

I. THREE-COMPONENT PLASMAS

The aim of the present paper is to develop a simple diagnostic tool to be used in the analysis of X-ray Thomson scattering from a three-component plasma formed by heating and compressing a compound composed of two distinct atoms. In recent years X-ray scattering experiments have been made on three-component CH [1–5] and LiH [6, 7] plasmas and used to determine temperatures, densities, ionization balance and mean ionic charges, together with information on static and dynamic structure factors. The theory of Thomson scattering from two-component plasmas consisting of a single ionic specie and electrons is laid out by Chihara [8]. Here, we follow the multi-component extension of Chihara's analysis given by Wünch et al. [9] using input parameters from an average-atom model of the plasma.

In the following paragraphs, we generalize the average-atom model described in Refs. [10, 11] to determine properties of a three-component plasma formed from ions having nuclear charges Z_1 and Z_2, atomic weights A_1 and A_2, and occupation numbers N_1 and N_2. The occupation numbers N_1 and N_2 are related to the ionic concentrations in the plasma x_1 and x_2 by $x_i = N_i/(N_1 + N_2)$, $i = 1, 2$.

In the average-atom model for a single ion type, the plasma is divided into neutral Wigner-Seitz (WS) cells consisting of a nucleus of charge Z and Z bound and continuum electrons. The continuum electron density $n_c(r)$ inside the WS cell merges into the uniform free-electron density n_e outside the cell boundary. To maintain neutrality, a uniform positive charge of density n_e is introduced. (One can imagine the smeared out charge of surrounding ions.) The picture that emerges is of a single average atom floating in a neutral sea of free electrons and positive ions. It is this picture that we want to generalize to molecules.

In the generalized average-atom model, the plasma is again divided into neutral WS cells, each consisting of a molecule and $N_1Z_1 + N_2Z_2$ electrons. The volume of the cell is

$$V = \frac{A}{\rho N_A}, \tag{1}$$

where N_A is Avogadro's number, $A = N_1A_1 + N_2A_2$ is the molecular weight and ρ is the plasma density. In the plasma, bonds are broken and molecules split up into individual ions and electrons; therefore, in the generalized version of average-atom model, the molecular WS cell splits into individual ionic cells. The WS cell for ion i contains a single ion with nuclear charge Z_i and Z_i electrons. It follows that

$$\frac{A}{\rho N_A} = N_1\frac{A_1}{\rho_1 N_A} + N_2\frac{A_2}{\rho_2 N_A}. \tag{2}$$

The individual atomic densities ρ_i, $i = 1, 2$ in Eq. (2) are yet to be determined. As noted above, the density of continuum electrons inside each WS cell in the average-atom

*Electronic address: johnson@nd.edu

model merges smoothly into the free-electron density n_e outside the cell. In the generalization of the average-atom model, we therefore require that the densities ρ_1 and ρ_2 be chosen so that the free-electron density associated with each individual ionic cell is the common free-electron density of the plasma n_e:

$$n_e(\rho_1) = n_e(\rho_2) = n_e. \tag{3}$$

Eqs. (2) and (3) are solved to give the ionic mass densities ρ_1 and ρ_2 and the free electron number density n_e.

The free-electron density is given in terms of the chemical potential μ by

$$n_e = \frac{2}{(2\pi)^3}\int d^3p\, f(p,\mu), \tag{4}$$

where

$$f(p,\mu) = \frac{1}{1+\exp[(p^2/2-\mu)/k_BT]} \tag{5}$$

is the free-electron Fermi distribution function. Eqs. (3-4) ensure that the plasma has a unique chemical potential. Note that atomic units (a.u.) in which $e = m_e = \hbar = 1$ are used here, with 1 a.u. in energy equal to 2 Rydbergs equal to 27.2 eV and 1 a.u. in length equal to 1 Bohr radius equal to 0.529 Å.

The number of free electrons inside the jth atomic cell is $Z_j^* = n_e V_j$, where V_j is the cell volume for the jth ionic type. The number of free electrons Z^* per molecular cell (volume V) is, correspondingly,

$$Z^* = n_e V = n_e(N_1V_1 + N_2V_2) = N_1Z_1^* + N_2Z_2^*. \tag{6}$$

The model developed above is applied to a warm dense CH plasma in Sec. III.

II. X-RAY THOMSON SCATTERING

The cross section for Thomson scattering of a photon with initial energy and momentum $(\omega_0, \boldsymbol{k}_0)$ to a final state with photon energy and momentum $(\omega_1, \boldsymbol{k}_1)$ is proportional to the dynamic structure factor $S(k,\omega)$, where $\omega = \omega_0 - \omega_1$, and $k = |\boldsymbol{k}_0 - \boldsymbol{k}_1|$.

There are three distinct contributions to $S(k,\omega)$: inelastic scattering by free electrons in the plasma $S_{ee}(k,\omega)$, inelastic scattering by bound electrons $S_b(k,\omega)$ and elastic scattering by ions $S_{ii}(k,\omega)$. In the present calculation, we normalize the theoretical structure factor to a molecular cell of volume $V = N_1V_1 + N_2V_2$.

The free-electron contribution to the structure factor associated with an ion of type i which is given by [8]

$$S_{ee}[\text{ion } i](k,\omega) = -\frac{1}{1-\exp(-\omega/k_BT)}\frac{Z_i^*k^2}{4\pi^2n_e}\text{Im}\left[\frac{1}{\epsilon(k,\omega)}\right], \tag{7}$$

is proportional to the imaginary part of the inverse of the dielectric function $\epsilon(k,\omega)$. The free-electron dielectric function $\epsilon(k,\omega)$ depends only on the chemical potential and temperature and is otherwise independent of the plasma composition. Here, we follow Gregori et al. [12] and evaluate $\epsilon(k,\omega)$ in the random-phase approximation. (See Ref. [11] for details). The sum of contributions to $S_{ee}(k,\omega)$ from N_1 ions of type 1 and N_2 ions of type 2 is proportional to the total ionic charge of the molecule:

$$S_{ee}(k,\omega) = N_1S_{ee}[\text{ion 1}] + N_2S_{ee}[\text{ion 2}] = -\frac{1}{1-\exp(-\omega/k_BT)}\frac{Z^*k^2}{4\pi^2n_e}\text{Im}\left[\frac{1}{\epsilon(k,\omega)}\right], \tag{8}$$

Since $Z^*/n_e = V$, S_{ee} is proportional to the molecular WS cell volume or inversely proportional to the plasma mass density.

The contribution to the dynamic structure factor from bound-electrons, as shown in Ref. [11], is given by

$$S_b(k,\omega) = \sum_{nl} S_{nl}(k,\omega), \tag{9}$$

where

$$S_{nl}(k,\omega) = \frac{o_{nl}}{2l+1}\sum_m \int \frac{p\, d\Omega_p}{(2\pi)^3} \times \left|\int d^3r\, \psi_{\boldsymbol{p}}^\dagger(\boldsymbol{r})\, e^{i\boldsymbol{k}\cdot\boldsymbol{r}}\, \psi_{nlm}(\boldsymbol{r})\right|^2. \tag{10}$$

In the above equation, $\psi_{nlm}(\boldsymbol{r})$ is the wave function for a bound-state electron with principal and angular quantum numbers n, l, m, occupation number o_{nl} and energy ϵ_{nl}, and $\psi_{\boldsymbol{p}}^\dagger(\boldsymbol{r})$ is a continuum wave function normalized to approach a plane wave of momentum $\boldsymbol{p}$ plus incoming spherical wave asymptotically. The energies of the bound-state and continuum electrons are of course related by $\epsilon_p = \omega + \epsilon_{nl}$.

The elastic scattering contribution to the dynamic structure factor is expressed in terms of the static structure factor $S(k)$,

$$S_{ii}(k,\omega) = S(k)\ \delta(\omega). \tag{11}$$

The static structure factor $S(k)$, in turn, is evaluated with the aid of a two-component model of the plasma in which partial contributions $S_{ij}(k)$ from interactions between ions of types i and j are treated directly and electron-ion interactions are treated indirectly as screening corrections to the ion-ion interaction potentials. From Eq.(A7) in Appendix A, we find

$$S(k) = N\left[x_1|f_1(k)|^2S_{11}(k) + x_2|f_2(k)|^2S_{22}(k) + 2\sqrt{x_1x_2}|f_1(k)||f_2(k)|S_{12}(k)\right], \tag{12}$$

where $N = N_1 + N_2$ and $x_i = N_1/N$. The functions $f_i(k)$ are Fourier transforms of the (bound + continuum) electron densities for ions of type i. The partial structure

TABLE I: Results of Average-Atom and Thomas-Fermi calculations for a CH plasma with free-electron density $n_e = 1.4 \times 10^{24}$ /cc at temperature $T = 10$ eV. The plasma and constituent densities ρ (gm/cc), cell volumes V (a.u.), ionic charges Z^*, number of bound electrons/cell N_b and number of continuum electrons/cell N_c are listed. The plasma chemical potential is 43.67 eV.

	Average-Atom			Thomas-Fermi		
	CH	C	H	CH	C	H
ρ	8.896	10.462	3.201	8.000	9.305	2.996
V	16.401	12.864	3.536	18.238	14.463	2.996
Z^*	3.403	2.669	0.734	3.775	2.996	0.779
N_b	2	2	0			
N_c	5	4	1			

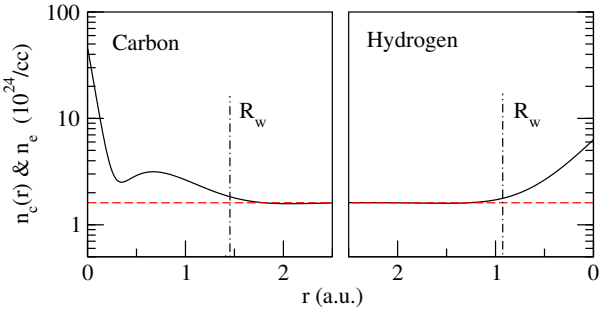

FIG. 1: Continuum electron density $n_c(r)$ (solid back lines) and free electron density n_e (dashed red line) for carbon and hydrogen in units 10^{24}/cc. Note that the densities are plotted inward from the ionic centers located at the boundaries. Radii of the Wigner-Seitz cells are designated by R_W. The continuum densities $n_c(r)$ merge smoothly into the common free-electron density n_e outside the respective WS cells.

factors $S_{ij}(k)$ above are evaluated in the hypernetted-chain approximation with exponentially damped interaction potentials as described in Appendix B.

It should be noted that the expressions for the individual contributions to the Thomson scattering cross section written out in this section differ from those derived in Ref. [9] only in overall normalization. The structure factor per molecule ($N_1 + N_2$ ions) is considered here, whereas the cross section per ion is given in [9].

III. APPLICATION TO CH

As a specific example, we consider a dense CH plasma at temperature $T = 10$ eV and free electron density $n_e = 1.4 \times 10^{24}$ /cc. These conditions are chosen for later comparison with X-ray Thomson scattering measurements on a shock-compressed CH plasma by Fletcher et al. [5].

The solution to Eqs. (2-3) that gives $n_e = 1.4 \times 10^{24}$ /cc at $T = 10$ eV using input from an average atom code is obtained by iteration. The resulting value of the plasma density is $\rho = 8.896$ gm/cc and the resulting value of the chemical potential is $\mu = 43.67$ eV. Data for individual C and H ions obtained in the average-atom calculation are given in the columns on the left in Table I. The carbon ion has a filled K-shell and four continuum electrons inside a WS cell of radius $R_W = 1.454$ a.u. and the hydrogen ion has a single continuum electron inside a WS sphere of $R_W = 0.9451$ a.u.. The corresponding data obtained using a temperature-dependent Thomas-Fermi (TF) calculation is listed in the columns on the right in Table I. The plasma density predicted by the TF calculation is 11% smaller than that predicted by the average-atom calculation, while the molecular Z^* is 11% larger.

The continuum density inside each sphere $n_c(r)$ merges smoothly into the free-electron density n_e outside the respective spheres. This behavior is illustrated in Fig. 1, where we plot $n_c(r)$ for C and H ions along with the free-electron density n_e. The effective charges per ion Z_i^* are listed in the third row of Table I. It should be emphasized that the average-atom model predicts that hydrogen has no bound electrons and that only K-shell electrons are bound in carbon under the present conditions of temperature and density.

For applications of average-atom models to Thomson scattering, it is important to distinguish between Z^*, which is the number of free electrons per ion, and N_c, which is the number of continuum electrons per ion inside the WS sphere. Thus, for carbon, the present average atom model predicts that there are $N_c = 4$ continuum electrons inside each WS cell but $Z^* = 2.669$, while for hydrogen, $N_c = 1$ but $Z^* = 0.734$. The reason for these differences can be seen in Fig. 1: continuum electrons inside the WS sphere pile up near the ionic nuclei, whereas free electrons are distributed uniformly. Indeed, if we subtract out the free-electron contribution from the charge density inside the WS sphere, we find from the average-atom normalization condition (Eq. 10 of Ref. [11]) that

$$Z - 4\pi \int_0^{R_W} r^2 \left[n(r) - n_e \right] dr = Z - (Z - Z^*) = Z^*. \quad (13)$$

From this equation, it follows that Z^* can also be interpreted as the ionic charge and therefore as the mean charge of the smeared out ionic background.

It should be noted that there is still a debate over whether to use Z^* (3.403 in this case) or the total number of continuum electrons N_c (5 in this case) as the multiplier in Eq. (8) for the S_{ee} term. However, using N_c does mean that the electron density is not the same for each ion unless we define volumes differently. A very complete recent discussion of mean ionization states in various atom-in-cell plasma models is given by Murillo et al. [13].

IV. THOMSON SCATTERING FROM CH

In Ref. [5], spectra of 9 keV X-rays scattered at angle $\theta = 135°$ from a shock-compressed CH capsule were measured. Relative intensities of scattered X-rays were obtained in the interval $8 - 10$ keV. Here, we model the 3.4 ns spectrum illustrated in Fig. 3 of Ref. [5], for which the temperature and electron density were determined to be $T = 10$ eV and $n_e = 1.4 \times 10^{24}$ /cc. The dynamic structure factor $S(k, \omega)$, for a fixed scattering angle θ, is only weakly dependent on k and, in the present paper, is evaluated at the elastic scattering value $k = 2k_0 \sin(\theta/2)$.

a. Inelastic Scattering The present result for $S_{ee}(k, \omega)$, which was obtained from Eq. (7) with Z_i/n_e replaced by V, is shown by the dashed red line in the Fig. 2. The dielectric function $\epsilon(k, \omega)$, which appears in the expression for $S_{ee}(k, \omega)$, depends on the plasma chemical potential μ and was evaluated in the random-phase approximation. The contribution to the inelastic scattering spectrum from $S_b(k, \omega)$, which is entirely from scattering by the K-shell electrons in carbon, was calculated from Eq. (10) using the bound and continuum wave functions from the carbon average-atom. The result is shown by the dot-dashed green line in Fig. 2.

b. Elastic Scattering The static structure factor $S(k)$ is evaluated using the expression given in Eq. (12) for a two-component plasma consisting of ions only. The partial structure factors $S_{ij}(k)$ are obtained by solving the Ornstein-Zerniky – hypernetted-chain (OZ-HNC) equations, which are written out in Appendix B. These equations depend on knowledge of the ion-ion interaction potential energy $V_{ij}(r)$, In the present example, we assume screened Coulomb interactions between ions

$$V_{ij}(r) = \frac{Z_i^* Z_j^*}{r} e^{-\kappa r}, \tag{14}$$

where κ is determined by the relation [14]

$$\kappa^2 = \frac{4}{\pi} \int_0^\infty dp f(p, \mu). \tag{15}$$

For the case at hand, $\kappa = 1.490$ a.u.. Plots of the three partial structure factor $S_{ij}(k)$ for $k \leq 10$ a.u. are shown in Fig. 3. The dot-dashed vertical line is at the elastic scattering value $k = 4.46$ a.u.. At this value of k, one finds: $S_{11}(k) = 1.033$, $S_{22}(k) = 0.933$ and $S_{12}(k) = -0.002$. Combining the above numbers in Eq. (12), we obtain $S(k) = 1.586$. The δ-function in Eq. (11) is represented by a Gaussian with full-width at half maximum of 100 eV. (The Gaussian width was inferred from the experimental spectrum). The resulting elastic-scattering contribution to the dynamic structure factor is shown as the thin blue curve in Fig. 2.

Experimental data from Fletcher et al. [5], shown by black dots in Fig. 2, is scaled to match the theoretical calculation of the total scattering factor $S(k, \omega)$, shown by the solid black curve, at the inelastic scattering peak. To align the theoretical inelastic peak with the corresponding experimental peak, the value of k used in $S_{ee}(k, \omega)$ was reduced by 10%. Such a reduction could be accounted for by a 15% reduction in the value of the scattering angle, which could be due to the experimental uncertainty in the scattering angle. Moreover, to achieve a match between theory and experiment, the value of the elastic scattering structure factor $S(k)$ was increased from the theoretical value by 20%, leaving us with an inconsistency between theoretical values of elastic and inelastic contributions to $S(k, \omega)$. Within the framework of the present model, one can scale the experimental intensity to agree with either inelastic or elastic components of the theory, but not both. We choose to scale the experiment to agree with the inelastic scattering components of the theory and find that the elastic amplitude $S(k)$ must be increased by 20% to match experiment.

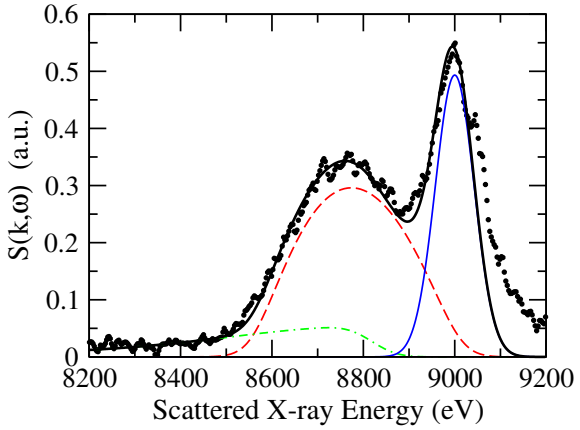

FIG. 2: Dynamic structure factor $S(k, \omega)$ for scattering of a 9 keV X-ray by a CH plasma at $T = 10$ eV and $N_e = 1.4 \times 10^{24}$ /cc from the present model are compared with the experimental 34ns spectrum from Ref. [5], represented by black dots and scaled to match the theory at the inelastic peak. Dashed red line $S_{ee}(k, \omega)$; dashed green line $S_b(k, \omega)$; thin blue line $S_{ii}(k, \omega)$; solid black line, $S(k, \omega)$.

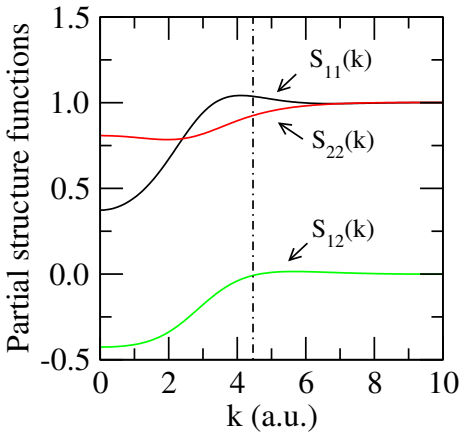

FIG. 3: Partial structure factors S_{ij} for a CH plasma at temperature $T = 10$ eV and electron density $n_e = 1.4 \times 10^{24}$ /cc. The dot-dashed vertical line is drawn at the experimental value of k.

Summary and Conclusions

A simple and easily implemented model for a three-component plasma with two ionic species and free electrons is developed. The model is based on the average-atom picture, in which all ions of a specific type are assumed to be identical and confined to identical Wigner-Seitz cells. Given the plasma density, temperature and composition, the model predicts the density, cell volume, and ionic charge of each ion. Moreover, the model gives wave functions for bound and continuum states and bound-state energies for each ionic type. The continuum density inside each WS cell merges into a cell-independent free-electron density n_e outside the cell. The fact that free-electron density is independent of the ionic type ensures that the plasma has a unique chemical potential μ.

The model is used to predict the X-ray Thomson scattering dynamic structure function. Very little information from the average-atom model is actually required in the Thomson scattering calculation. The dominant features seen in the experimental X-ray spectrum shown in Fig. 2 are the elastic scattering peak at 9000 eV and the broad down-shifted shoulder from scattering by free electrons. The RPA expression for the free-electron scattering structure factor $S_{ee}(k,\omega)$, for given values of k and ω, depends only on ratio μ/T of the chemical potential to the temperature T. Although the ionic charges Z_i^* appear in Eq. (7), the total contribution from both ionic species is independent of Z_i^* and is proportional to normalization volume V. Indeed, any atom-in-cell model of the plasma, adjusted to give specific values of n_e and temperature T, is guaranteed to give the same value of μ by virtue of Eq. (4). Thus, for example, the Thomas-Fermi model of the CH plasma leads to a value of $S_{ee}(k,\omega)$ that has precisely the same shape as the average atom value, but has an amplitude 11% larger, reflecting the smaller CH density inferred from the Thomas-Fermi calculation, as shown in Table I.

The bound-state contribution $S_b(k,\omega)$, which is important at the low-frequency end of the spectrum, requires quantum mechanical calculations of both bound and continuum (distorted-wave) wave functions in order to obtain a quantitatively accurate understanding of the low-frequency tail of the spectrum. This need for accurate bound-free matrix elements for applications to plasma diagnostics was emphasized recently by Mattern and Seidler [15].

Finally, the static structure factor $S(k)$ depends on input from the average-atom model in two distinct ways: (1) through the form factors of the ions $f_i(k)$ defined in Eq. (A1), which require a knowledge of the bound-state wave functions, and (2) through effective charges Z_i^* in the interaction potentials given in Eq. (14). The use of screened Coulomb potentials in the evaluation of $S(k)$ is the weakest part of the present analysis and improving the interaction potentials within the average-atom framework is the goal of ongoing research.

Acknowledgements

The authors owe a debt of gratitude to L. Fletcher and S. H. Glenzer for providing the experimental data in Fig. 2. We also thank G. Zimmerman for helping us to understand ion mixtures and K. T. Cheng for helpful discussions. The work of J.N. was performed under the auspices of the U.S. Department of Energy by Lawrence Livermore National Laboratory under Contract DE-AC52-07NA27344.

[1] G. Gregori, S. Glenzer, H. Chung, D. Froula, R. Lee, N. Meezan, J. Moody, C. Niemann, O. Landen, B. Holst, et al., J. Quant. Spectros. Radiat. Transfer **99**, 225 (2006).
[2] H. Sawada, S. P. Regan, D. D. Meyerhofer, I. V. Igumenshchev, V. N. Goncharov, T. R. Boehly, T. C. S. R. Epstein, V. A. Smalyuk, B. Yaakobi, G. Gregori, et al., Phys. Plasmas **14**, 122703 (2007).
[3] B. Barbrel, M. Koenig, A. Benuzzi-Mounaix, E. Brambrink, C. Brown, D. O. Gericke, B. Nagler, M. Rabec le Gloahec, D. Riley, C. Spindloe, et al., Phys. Rev. Letts. **102**, 165004 (2009).
[4] G. Hu, X. Zhang, J. Zheng, A. Lei, B. Shen, Z. Xu, J. Zhang, J. Yang, G. Yang, M. Wei, et al., Plasma Science and Technology **14**, 864 (2012).
[5] L. Fletcher, A. Kritcher, A. Pak, T. Ma, T. Döppner, C. Fortmann, L. Divol, O. Landen, J. Vorberger, D. Chapman, et al., Phys. Plasmas **20**, 056316 (2013).
[6] A. L. Kritcher, P. Neumayer, J. Castor, T. Döppner, R. W. Falcone, O. L. Landen, H. J. Lee, R. W. Lee, E. C. Morse, A. Ng, et al., Science **322**, 69 (2008).
[7] A. L. Kritcher, P. Neumayer, C. Brown, P. Davis, T. Döppner, R. Falcone, D. O. Gericke, G. Gregori, B. Holst, O. L. Landen, et al., Phys. Rev. Letts. **103**, 245004 (2009).
[8] J. Chihara, J. Phys.: Condens. Matter **12**, 231 (2000).
[9] K. Wünch, J. Vorberger, G. Gregori, and G. Gericke, EPL **94**, 25001 (2011).
[10] W. R. Johnson, C. Guet, and G. F. Bertsch, J. Quant. Spectros. & Radiat. Transfer **99**, 327 (2006).
[11] W. Johnson, J. Nilsen, and K. Cheng, Phys. Rev. E **86**, 036410 (2012).
[12] G. Gregori, S. H. Glenzer, W. Rozmus, R. W. Lee, and O. L. Landen, Phys. Rev. E **67**, 026412 (2003).
[13] M. S. Murillo, J. Weisheit, S. B. Hansen, and M. W. C. Dharma-wardana, Phys. Rev. E **87**, 063113 (2013).
[14] K. Wünsch, P. Hilse, M. Schlanges, and D. O. Gericke, Phys. Rev. E **77** (2008), ISSN 1539-3755.
[15] B. Mattern and G. Seidler, Phys. Plasmas **20**, 022706 (2013).
[16] L. S. Ornstein and F. Zernike, Phys. Z. **19**, 134 (1918).
[17] J. P. Hansen and I. R. McDonald, *Theory of Simple Liquids* (Academic Press, 2009).

Appendix A: Static Structure Factor

The static structure factor for elastic scattering from a single average-atom is $S(\boldsymbol{k}) = |f(k)|^2$ where,

$$f(k) = \int d^3r\, n(r)\; e^{i\boldsymbol{k}\cdot\boldsymbol{r}}, \tag{A1}$$

with $n(r) = n_b(r) + n_c(r)$ being the (bound+continuum) electron density inside the WS sphere. Note that $f(k)$ is real for a spherically symmetric charge density. The generalization to a macroscopic system containing N_1 identical ions of type 1 and N_2 identical ions of type 2 is

$$S(\boldsymbol{k}) = \left[|f_1(k)|^2 \sum_{a=1}^{N_1}\sum_{b=1}^{N_1} e^{i\boldsymbol{k}\cdot(\boldsymbol{R}_{1b}-\boldsymbol{R}_{1a})} + (1\to 2)\right] + \left[f_1(k) f_2^*(k) \sum_{a=1}^{N_1}\sum_{b=1}^{N_2} e^{i\boldsymbol{k}\cdot(\boldsymbol{R}_{2b}-\boldsymbol{R}_{1a})} + (1\leftrightarrow 2)\right] \tag{A2}$$

where, for example, $\boldsymbol{R}_{ia}$ is the coordinate of the a-th ion of type i. For a homogeneous isotropic distribution of particles, the double sum over type 1 ions can be simplified to

$$\sum_{a=1}^{N_1}\sum_{b=1}^{N_1} e^{i\boldsymbol{k}\cdot(\boldsymbol{R}_{1b}-\boldsymbol{R}_{1b})} \to N_1\left(1 + n_1\int d^3r\, g_{11}(r)\, e^{i\boldsymbol{k}\cdot\boldsymbol{r}}\right), \tag{A3}$$

where n_1 is the number density of type 1 ions and $g_{11}(r)$ is a partial pair distribution function. Generally, $g_{ij}(r)\, d^3r$ is the probability of type i particles being in d^3r at a distance r from a given particle of type j. Note that $\lim_{r\to\infty} g_{ij}(r) = 1$. Clearly, $g_{ij} = g_{ji}$.

The sum over ions of type 2 on the first line of Eq. (A2) can be similarly rewritten in terms of n_2 and $g_{22}(r)$. Following this pattern, the sum on the third line of (A2) may be written

$$\sum_{a=1}^{N_1}\sum_{b=1}^{N_2} e^{i\boldsymbol{k}\cdot(\boldsymbol{R}_{2b}-\boldsymbol{R}_{1a})} \to N_1 n_2\int d^3r\, g_{21}(r)\, e^{i\boldsymbol{k}\cdot\boldsymbol{r}}, \tag{A4}$$

and its conjugate as

$$\sum_{b=1}^{N_2}\sum_{a=1}^{N_1} e^{i\boldsymbol{k}\cdot(\boldsymbol{R}_{1a}-\boldsymbol{R}_{2b})} \to N_2 n_1\int d^3r\, g_{12}(r)\, e^{i\boldsymbol{k}\cdot\boldsymbol{r}}. \tag{A5}$$

The coefficients of the above two integrals are equal: $N_1 n_2 = N_2 n_1 = N_1 N_2/V = x_1 x_2 N n$, where $N = N_1 + N_2$ and $n = n_1 + n_2$.

For numerical purposes, it is necessary to subtract the asymptotic value of g_{ij} in the above integrals. Thus

$$\int d^3r\, g_{ij}(r)\, e^{i\boldsymbol{k}\cdot\boldsymbol{r}} = \int d^3r\, (g_{ij}(r) - 1)\, e^{i\boldsymbol{k}\cdot\boldsymbol{r}} + (2\pi)^3\delta(\boldsymbol{k}). \tag{A6}$$

The function $\delta(\boldsymbol{k})$ contributes to $S(k)$ only in the forward direction and can be safely ignored in our calculations.

With the above relations in mind, we find that the static structure factor per molecule with $N = N_1 + N_2$ ions is

$$S(k) = N\sum_{i=1}^{2}\sum_{j=1}^{2}\sqrt{x_i x_j}\, f_i(k)\, f_j(k) S_{ij}(k), \tag{A7}$$

where

$$S_{ij} = \delta_{ij} + \sqrt{n_i n_j}\int d^3r\, (g_{ij}(r) - 1)\, e^{i\boldsymbol{k}\cdot\boldsymbol{r}}. \tag{A8}$$

Appendix B: OZ-HNC Equations

From Eq. (A8), it follows that the partial structure factors for a plasma with two ionic species are

$$S_{ij}(k) = \delta_{ij} + \sqrt{n_i n_j}\,\frac{4\pi}{k}\int_0^\infty r\sin kr\, h_{ij}(r)\, dr, \tag{B1}$$

where $h_{ij}(r) = g_{ij}(r) - 1$ defines the "total" two-particle correlation function for particles of types i and j. The total correlation functions $h_{ij}(r)$ are related to the "direct" correlation functions $c_{ij}(r)$ by the Ornstein-Zernike (OZ) equations [16]:

$$h_{ij}(\boldsymbol{r}) = c_{ij}(r) + \sum_l n_l\int c_{il}(\boldsymbol{r}-\boldsymbol{r}')h_{lj}(\boldsymbol{r}')d^3r'. \tag{B2}$$

The pair distribution functions $g_{ij}(r)$ can be determined from the interaction potentials $V_{ij}(r)$ through the hypernetted-chain (HNC) closure relation [17, Sec. 10.2]

$$g_{ij}(r) = \exp\left(-\beta V_{ij}(r) + h_{ij}(r) - c_{ij}(r)\right), \tag{B3}$$

where $\beta = 1/(k_{\rm B}T)$. Introducing the "indirect" correlation functions $t_{ij}(r) = h_{ij}(r) - c_{ij}(r)$, one can rewrite the HNC relation as

$$c_{ij}(r) = \exp\left(-\beta V_{ij}(r) + t_{ij}(r)\right) - t_{ij}(r) - 1. \tag{B4}$$

The Fourier transforms of the (OZ) equations for a multi-component plasma may be written

$$\sum_l \left[\delta_{lj} - n_l\,\hat{c}_{il}(k)\right]\hat{t}_{lj}(k) = \sum_l n_l\,\hat{c}_{il}(k)\,\hat{c}_{lj}(k), \tag{B5}$$

where we have introduced the notation $\hat{c}_{ij}(k)$ and $\hat{t}_{ij}(k)$ to designate the Fourier transforms of $c_{ij}(r)$ and $t_{ij}(r)$, respectively. For a plasma with two ionic components, these equations are rearranged to give $\hat{t}_{ij}(k)$ in terms of $\hat{c}_{kl}(k)$,

$$\hat{t}_{11} = \left[n_2\,(1 + n_1\,\hat{c}_{11})\hat{c}_{12}^2 + n_1\,(1 - n_2\,\hat{c}_{22})\hat{c}_{11}^2\right]/d \tag{B6}$$

$$\hat{t}_{22} = \left[n_1\,(1 + n_2\,\hat{c}_{22})\hat{c}_{12}^2 + n_2\,(1 - n_1\,\hat{c}_{11})\hat{c}_{22}^2\right]/d \tag{B7}$$

$$\hat{t}_{12} = \hat{c}_{12}\left[n_1\,\hat{c}_{11} + n_2\,\hat{c}_{22} - n_1 n_2\,(\hat{c}_{11}\hat{c}_{22} - \hat{c}_{12}^2)\right]/d \tag{B8}$$

$$d = 1 - n_1\,\hat{c}_{11} - n_2\,\hat{c}_{22} + n_1 n_2\,(\hat{c}_{11}\hat{c}_{22} - \hat{c}_{12}^2). \tag{B9}$$

Starting with the approximation $\hat{t}_{ij}(k) = 0$, one evaluates $\hat{c}_{ij}(k)$ from the Fourier transform of Eq. (B4) and continues the iteration procedure using Eqs. (B6-B9). Typically 20 iterations are required to achieve 8 figure accuracy.